Article

Variations in Remotely-Sensed Phytoplankton Size Structure of a Cyclonic Eddy in the Southwest Indian Ocean

Tarron Lamont [1,2,*], Raymond G. Barlow [2,3] and Robert J. W. Brewin [4,5]

[1] Oceans & Coasts Research, Department of Environmental Affairs, Private Bag X4390, Cape Town 8000, South Africa
[2] Marine Research Institute & Department of Oceanography, University of Cape Town, Private Bag X3, Rondebosch 7701, South Africa; rgb.barlow@gmail.com
[3] Bayworld Centre for Research & Education, 5 Riesling Road, Constantia, Cape Town 7806, South Africa
[4] Plymouth Marine Laboratory (PML), Prospect Place, The Hoe, Plymouth PL1 3DH, UK; robr@pml.ac.uk
[5] National Centre for Earth Observation, PML, Prospect Place, The Hoe, Plymouth PL1 3DH, UK
[*] Correspondence: tarron.lamont@gmail.com; Tel.: +27-21-819-5039

Abstract: Phytoplankton size classes were derived from weekly-averaged MODIS Aqua chlorophyll *a* data over the southwest Indian Ocean in order to assess changes in surface phytoplankton community structure within a cyclonic eddy as it propagated across the Mozambique Basin in 2013. Satellite altimetry was used to identify and track the southwesterly movement of the eddy from its origin off Madagascar in mid-June until mid-October, when it eventually merged with the Agulhas Current along the east coast of South Africa. Nano- and picophytoplankton comprised most of the community in the early phase of the eddy development in June, but nanophytoplankton then dominated in austral winter (July and August). Microphytoplankton was entrained into the eddy by horizontal advection from the southern Madagascar shelf, increasing the proportion of microphytoplankton to 23% when the chlorophyll *a* levels reached a peak of 0.36 mg·m^{-3} in the third week of July. Chlorophyll *a* levels declined to <0.2 mg·m^{-3} in austral spring (September and October) as the eddy propagated further to the southwest. Picophytoplankton dominated the community during the spring period, accounting for >50% of the population. As far as is known, this is the first study to investigate temporal changes in chlorophyll *a* and community structure in a cyclonic eddy propagating across an ocean basin in the southwest Indian Ocean.

Keywords: ocean colour; phytoplankton size structure; cyclonic eddy; Southwest Indian Ocean

1. Introduction

Observations in the Indian Ocean have demonstrated that flow around the southern tip of Madagascar is complex [1–3]. Previous studies have suggested that the southern branch of the East Madagascar Current (SEMC) bifurcates, with a portion of the flow retroflecting and persisting east [4,5], and the remainder of the flow continuing west across the northern part of the Mozambique Basin (MB) and feeding into the Agulhas Current system (Figure 1), mainly in the form of mesoscale eddies [6–10]. In contrast, a more recent investigation has shown that the SEMC flow dissolves into a series of cyclonic and anticyclonic dipole eddy pairs (Figure 1), and that there is no retroflection or westward jet [3]. Dipole pair formation occurs with a frequency of four to six per year, with most pairs breaking up shortly after formation and interacting with other mesoscale eddies [3]. However, recently it has been shown that the number of cyclonic eddies exceeds the anticyclonic eddies generated southwest of Madagascar [9]. Analysis of water mass characteristics of these dipolar structures has shown that the

cyclonic eddies consist of waters with Mozambique Channel (MC) properties, while the anticyclonic eddies are comprised of waters from the SEMC [6,11].
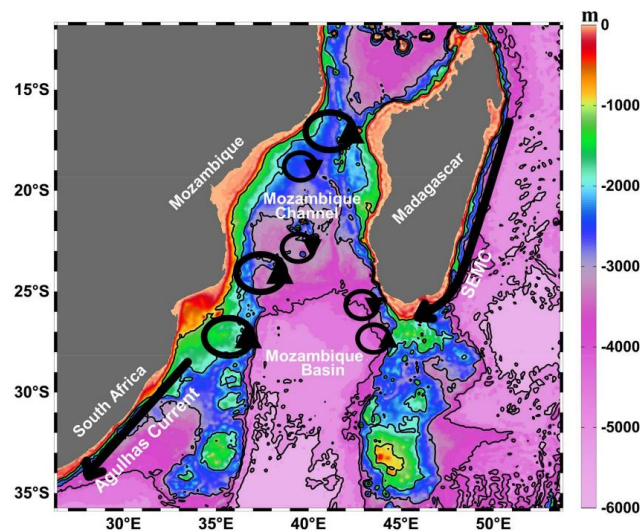
Figure 1. Main oceanographic features in the Mozambique Channel and Mozambique Basin. The southern branch of the East Madagascar Current (SEMC), the Agulhas Current, Mozambique Channel eddies, as well as dipoles stemming from the SEMC are indicated. Anticlockwise (clockwise) circulation features indicate anticyclonic (cyclonic) eddies. Black contours indicate the 1000 m, 2000 m, 3000 m, 4000 m, and 5000 m bathymetric contours.

It has been demonstrated that eddies in the southwest Indian Ocean have a significant influence on the structure of biological communities and on ecosystem functioning. Overall, it is typical to have elevated chlorophyll in cyclonic eddies, and lower concentrations in anticyclonic eddies [12–14]. However, there appear to be some differences in the characteristics of cyclonic eddies sampled during different seasons in the MC and MB. Cyclonic eddies studied during austral spring and summer in the MC exhibited shallow upper mixed layers and nitracline depths, and deep euphotic zones, with distinct subsurface chlorophyll maxima (SCM) being associated with the stratified conditions in the upper layers of these eddies [15]. In contrast, a cyclonic eddy studied during austral winter in the MB had a shallower euphotic zone, a deeper upper mixed layer and uniform chlorophyll profiles [15]. Another eddy sampled in the MB toward the end of winter showed a less pronounced SCM and roughly equal euphotic zone and upper mixed layer depths, suggesting a transition from a well-mixed upper layer during winter to stratified conditions in summer [15]. These observations suggest that during summer and winter, the isopycnal uplift associated with cyclonic eddies in the MC and MB elevates the nitracline and enables the development of SCMs, whereas in winter, stronger wind-driven mixing deepens the upper mixed layer and nitracline, despite the isopycnal uplift within cyclonic eddies [15].

During 17–23 July 2013, a more detailed investigation of the MB cyclonic eddy referred to above [16], indicated that the phytoplankton community comprised mainly haptophytes and diatoms, with prasinophytes, Prochlorococcus and pelagophytes also being prominent to the east and west of the eddy, as inferred from CHEMTAX analysis of pigment data [16]. There was little difference in community structure, chlorophyll *a* specific absorption at 440 nm, and pigment:chlorophyll *a* ratios between the surface and the SCM, reflecting acclimation to fluctuating light conditions in a well-mixed upper layer. Chlorophyll *c* and fucoxanthin:chlorophyll *a* ratios were elevated over most of the eddy, while 19′-hexanoyloxyfucoxanthin ratios increased in the eastern and western sectors. An increase in diadinoxanthin:chlorophyll *a* ratios and a decline in the quantum efficiency of photochemistry in photosystem II under high light conditions, indicated some photoprotection and photoinhibition at the surface, even in a well-mixed environment [16].

Satellite altimetry and ocean colour data was used to track the origin and development of the MB eddy in preparation for the in situ investigation during 17–23 July 2013 [15,16]. Satellite data continued to be observed during and after the research cruise in order to follow the movement of the eddy towards the Agulhas Current ecosystem over a 4 month period. The satellite chlorophyll data was useful to track changes in surface phytoplankton biomass across the MB, both spatially and temporally. The size distribution of phytoplankton communities plays a key role in the trophic structuring of ecosystems, where communities dominated by larger-sized phytoplankton usually have higher rates of photosynthesis and are able to export organic matter through shorter food chains, while ecosystems dominated by smaller-size phytoplankton are usually characterized by more complex food webs underpinned by stronger microbial activity and recycling of organic material [17]. Thus, observations of phytoplankton size structure are crucial to improve our understanding of marine ecology, biogeochemistry, and ecosystem functioning [17]. More detailed information on the size class composition of phytoplankton in the eddy can be obtained by applying the three-component model of Brewin et al. [18] that computes the fractional contributions of micro- (>20 μm), nano- (2–20 μm) and picophytoplankton (<2 μm) to the overall chlorophyll *a* concentration. The Brewin et al. [18] model has been retuned using in situ pigment data for application to the southern African marine region and used to investigate the changes in seasonal and monthly climatologies of phytoplankton size fractions in various sub-regions [19]. In this study, the retuned Brewin et al. [18] model was applied to satellite chlorophyll *a* data for the MB in order to track the fractional variability in phytoplankton size classes in the cyclonic eddy as it propagated towards the east coast of South Africa between June and October 2013. The objectives of the study are to: (1) track the total chlorophyll *a* within the eddy across the Basin to assess variability in phytoplankton biomass; (2) assess changes in the proportions of micro-, nano- and picophytoplankton in relation to seasonal progression through austral winter and spring.

2. Materials and Methods

2.1. Retuning of the Model

A comprehensive description of the retuning of the Brewin et al. [18] model is presented in Lamont et al. [19], together with the final model parameters and statistical assessment of model performance, therefore only a summary is presented here. The abundance-based model was developed by Brewin et al. [18] to estimate the chlorophyll *a* concentrations of three phytoplankton size classes (micro- (>20 μm), nano- (2–20 μm), and picophytoplankton (<2 μm)), as a function of the total chlorophyll *a* concentration (*C*). The model is based on the exponential functions of Sathyendranath et al. [20] where the chlorophyll concentration of picophytoplankton (C_p) and combined nano-picophytoplankton ($C_{p,n}$) are computed as:

$$C_p = C_p^m \left[1 - exp\left(S_p C \right) \right] \tag{1}$$

and

$$C_{p,n} = C_{p,n}^m \left[1 - exp\left(S_{p,n} C \right) \right] \tag{2}$$

where the parameters S_p and $S_{p,n}$ determine the initial slope between size-fractionated chlorophyll *a* and total chlorophyll *a* (denoted *C* in Equations (1) and (2)), and C_p^m and $C_{p,n}^m$ determine the asymptotic maximum values for the two size-classes. Nanophytoplankton chlorophyll *a* (C_n) and microphytoplankton chlorophyll *a* (C_m) are computed as $C_n = C_{p,n} - C_p$ and $C_m = C - C_{p,n}$. The fractions of each size class (F_p, F_n and F_m) are computed by dividing the size-fractionated chlorophyll *a* (C_p, C_n and C_m) by total chlorophyll *a* (*C*). Parameterization of the global model was performed by using coefficients determined from relationships between High Performance Liquid Chromatography (HPLC)-derived pigment biomarkers and total chlorophyll *a* and relating specific pigments to each size class according to Uitz et al. [21]. Further refinements followed those of

Brewin et al. [18] and Devred et al. [22]. The model has been applied to satellite data and extensively validated with a range of independent in situ data from various marine environments [18,23–25].

For application to the southwest Indian Ocean, the global model was regionally-tuned using in situ HPLC data from the southern African marine region as described by Lamont et al. [19] (also see Figure 2a–c). Only samples from the upper 20 m were used, and where the difference between chlorophyll *a* and total accessory pigments was <30% of the total pigment concentration. A total of 407 samples were available and included locations in the vicinity of Tanzania, the Mozambique Channel, Madagascar and South Africa, in addition to samples from the west and southwest of southern Africa. Size-fractionated chlorophyll *a* was computed as described by Brewin et al. [24], where total chlorophyll *a* concentration is calculated from the weighting of seven diagnostic pigments [21] and the chlorophyll *a* in each size class is then estimated. Picophytoplankton chlorophyll *a* (C_p) was estimated using zeaxanthin, total chlorophyll *b*, and allocating 19′-hexanoyloxyfucoxanthin to the picophytoplankton pool where total chlorophyll *a* concentrations were $\leq$0.08 mg·m^{-3}. Nanophytoplankton chlorophyll *a* (C_n) was estimated using 19′-hexanoyloxyfucoxanthin, 19′-butanoyloxyfucoxanthin, alloxanthin, and allocating some of the fucoxanthin to the nanophytoplankton pool according to Devred et al. [22]. Microphytoplankton chlorophyll (C_m) was estimated using peridinin and the remaining fucoxanthin that was attributed to the micro- size class [22,24]. Diagnostic pigments derived by HPLC do not provide direct measures of size but are instead used to infer size-fractionated chlorophyll *a*, and although these pigments can be found in a variety of different phytoplankton taxa and size classes [17], we have attempted to minimize these concerns by applying recent refinements to the pigment-based estimation of size classes [18,22].

In situ samples were matched to daily, level 3 satellite chlorophyll *a* data acquired from MODIS-Aqua (v2014.0) in both time and space, using a 3×3 pixel window following Bailey and Werdell [26]. The average chlorophyll *a* of the nine pixels was used as the satellite estimate, but only match-ups of five or more pixels were included to ensure homogeneity [24,26,27]. Following these criteria, only 33 satellite match-ups out of a possible 407 became available. The satellite match-ups were used for independent validation of satellite and size-fractionated chlorophyll *a*, leaving 374 samples for retuning of the Brewin et al. [18] model. Model performance was assessed using appropriate statistical tests in log$_{10}$ space for the chlorophyll *a* concentrations and in linear space for the size fractions. Equations (1) and (2) were fitted to the 374 samples using a standard, nonlinear, least-squares method with relative weighting to retrieve the model parameters presented in Table 1 and Figure 3b of Lamont et al. [19]. The in situ chlorophyll *a* data used for the model fit ranged from 0.03 to 30.6 mg·m^{-3}. The new model parameters were compared to the Atlantic and global models of Brewin et al. [18,24] and found to have significantly higher initial slopes, justifying a regional tuning of the model, and indicating a greater contribution of small cells at low total chlorophyll *a* values. The retuned model captures the general trends in absolute chlorophyll *a* concentration for each size fraction and the fractional proportion of the total chlorophyll *a* for the southern African dataset [19].

2.2. Satellite Data Analysis

Daily maps of Merged Absolute Dynamic Topography [28] were used to assess the movement and age of the cyclonic eddy as it propagated across the MB (Figure 3). The eddy was identified and tracked by means of an eddy detection technique that combines the use of the Okubo-Weiss parameter and closed Sea Surface Height (SSH) contours, as described by Halo et al. [8]. Standard weekly-averaged (8-day) chlorophyll *a* data from MODIS-Aqua (v2018.0), at 4.5 km spatial resolution [29] was used to investigate the variations in weekly-average chlorophyll *a*, as well as the fractional contributions of micro-, nano-, and picophytoplankton between 18 June and 15 October 2013. The dominance of the various size classes is usually associated with different chlorophyll *a* ranges, where microphytoplankton dominate at high chlorophyll *a*, nanophytoplankton at intermediate chlorophyll *a*, and picophytoplankton at low chlorophyll *a* concentrations [21,30,31]. The centre of the eddy was estimated from altimetry data by using the eddy detection technique described above [8],

and values of chlorophyll *a* and the fractional contributions were averaged in a 3 × 3 pixel window around this location.
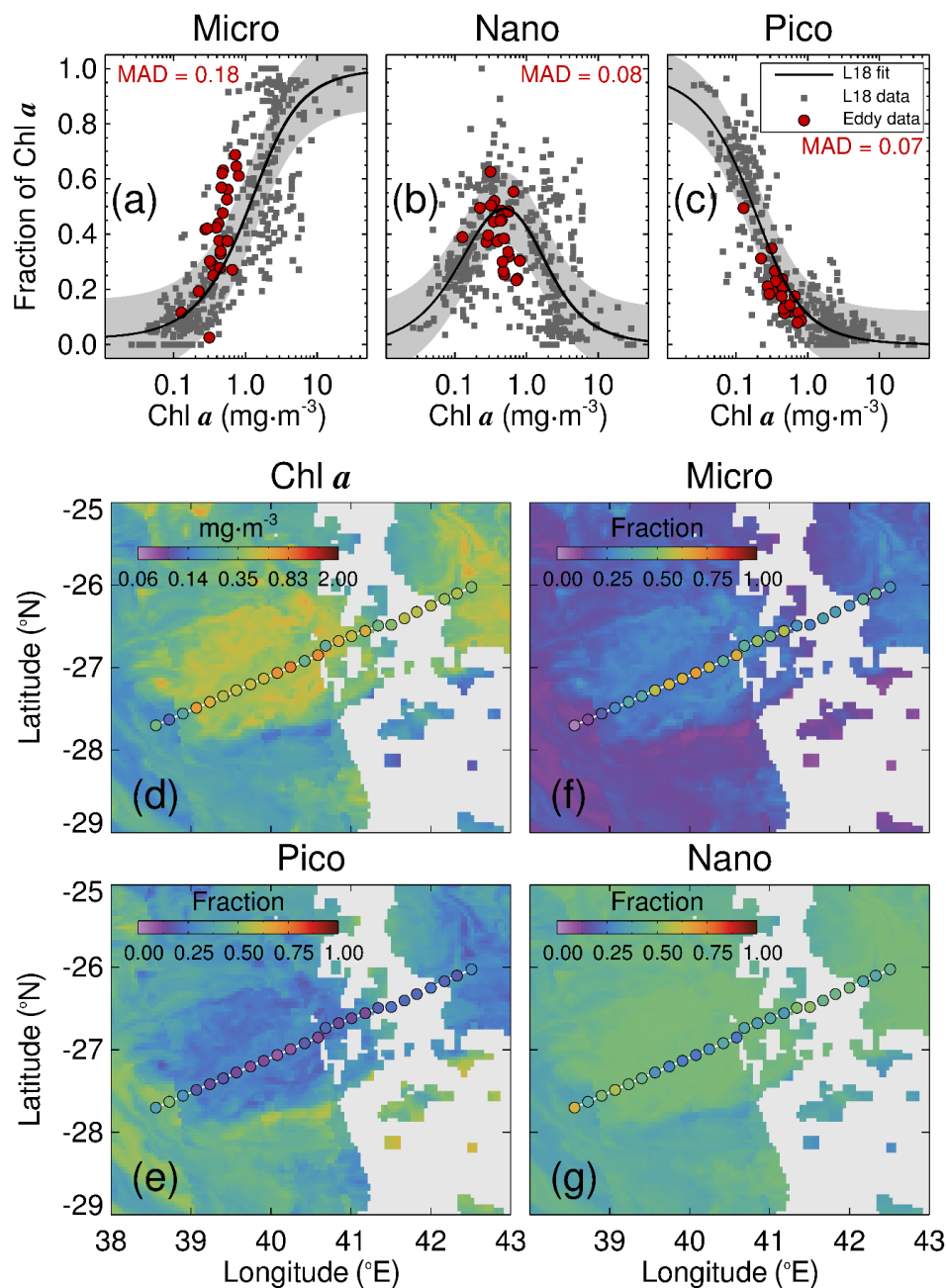
Figure 2. Verification of the use of the three-component model for studying phytoplankton size structure within the MB eddy. (**a**–**c**) show the fractions of micro-, nano-, and picophytoplankton, respectively, as a function of chlorophyll *a* for in situ measurements collected during the passage of the MB eddy with the three-component model overlain. For comparison, the data from the Lamont et al. [19] (L18) study is also shown, and the grey shading represents uncertainty in the fractions based on the validation in the L18 study (see their Figure 3). MAD is the median absolute difference between the model and the in situ size fractions from the MB eddy. (**d**–**g**) show the in situ chlorophyll *a* and size fractions overlain onto MODIS-Aqua estimates from 20 and 24 July 2013, merged (averaged) into a single image. The in situ samples are coloured on the same scale as the satellite images.
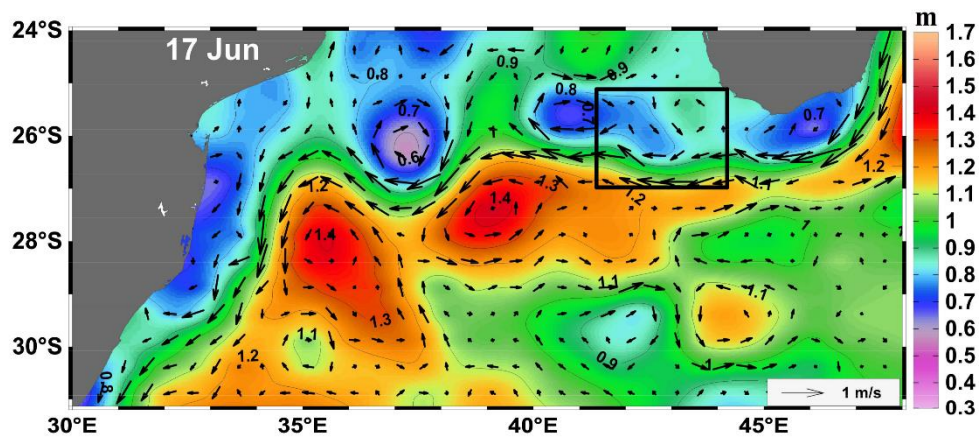
Figure 3. Sea Surface Height (colour contours) and geostrophic velocity (black arrows) over the Mozambique Basin on 17 June 2013. The black box highlights the location of the cyclonic eddy.

2.3. Model Verification

To verify the applicability of the re-tuned three-component model [19] for tracking the phytoplankton size structure in the MB eddy, we made use of a transect of HPLC data collected during the passage of the eddy between the 17 and the 23 of July 2013 [16]. This data is independent of the in situ data used by Lamont et al. [19] to re-tune the three-component model. The fractions of chlorophyll a in the three size classes of phytoplankton were estimated from HPLC data following the method described in Section 2.1. (see Brewin et al. [24] and Lamont et al. [19] for further details), consistent with the manner in which Lamont et al. [19] re-tuned the model. We also made use of the in situ fractions used in Lamont et al. [19] to parameterize the model, for comparison with the in situ data from the MB eddy (Figure 2a–c). Two relatively clear-sky MODIS-Aqua images (v2018, 4.5 km spatial resolution [29]) centered on the eddy (on the 20 and 24 of July 2013) were downloaded from the NASA website (https://oceancolor.gsfc.nasa.gov) and merged (averaged) into a single image, for comparison with the in situ observations (Figure 2d–g).

3. Results

The in situ size fractions collected in the MB eddy were found to lie within the range of the data used by Lamont et al. [19] for re-tuning the three-component model, for a given chlorophyll a concentration (Figure 2a–c). The median absolute differences (MAD) between modelled size fractions using in situ total chlorophyll a as input to Equation (1) and (2) and the actual in situ size fractions were <0.18, with slightly better performance for picophytoplankton (MAD = 0.07) than for nano- and microphytoplankton (MAD = 0.08 and 0.18, respectively), giving confidence in the application of the Lamont et al. [19] model to map size structure within the eddy. When overlaying the in situ chlorophyll a and size fractions from the transect [16] onto the satellite estimates from MODIS-Aqua, the satellite data was found to nicely capture the spatial variability in the in situ data (Figure 2d–g), especially when considering the mis-match in spatial and temporal scales between the two datasets (e.g., satellite data collected on the 20th and 24th, while in situ data was collected between the 17th and 23rd July). Lower fractions of picophytoplankton, higher fractions of microphytoplankton, and higher chlorophyll a within the eddy during this period, when compared with waters surrounding the eddy, were consistent between the two datasets.

The cyclonic eddy was first detected at 26.03°S; 42.82°E on 16 June 2013, where SSH was 0.76 m and geostrophic velocity vectors showed the beginning of circular flow as the eddy split from the larger cyclonic eddy to the west (Figure 3). By 21 June, SSH had decreased to ~0.69 m and geostrophic velocity increased as the emerging eddy moved further southeast to 25.90°S; 42.10°E (Figure 4a). The eddy was clearly distinguished as a separate feature by 29 June, with geostrophic velocities of 0.5–1 m·s^{-1}

and a minimum SSH of ~0.5 m and had moved southwest to 26.30°S; 41.60 °E (Figure 4b). The eddy continued propagating southwest and by 17–22 July, it was positioned at 27°S; 40.50°E (Figure 4c,d) and had a diameter of about 250 km, at which time it was sampled during the research cruise [15,16]. Figures 3 and 4a–d depict an apparent extension of the SEMC, with generally westerly flow from 17–29 June shifting to a more southwesterly direction by 17–22 July. However, it is more likely that this westerly to southwesterly flow resulted from the particular spatial structuring and interaction of the intense mesoscale eddy field to the southwest of Madagascar (Figures 3 and 4a–d). Of significance is the locality of the cyclonic eddy along the northern edge of this westerly to southwesterly flow (Figure 4a–d).
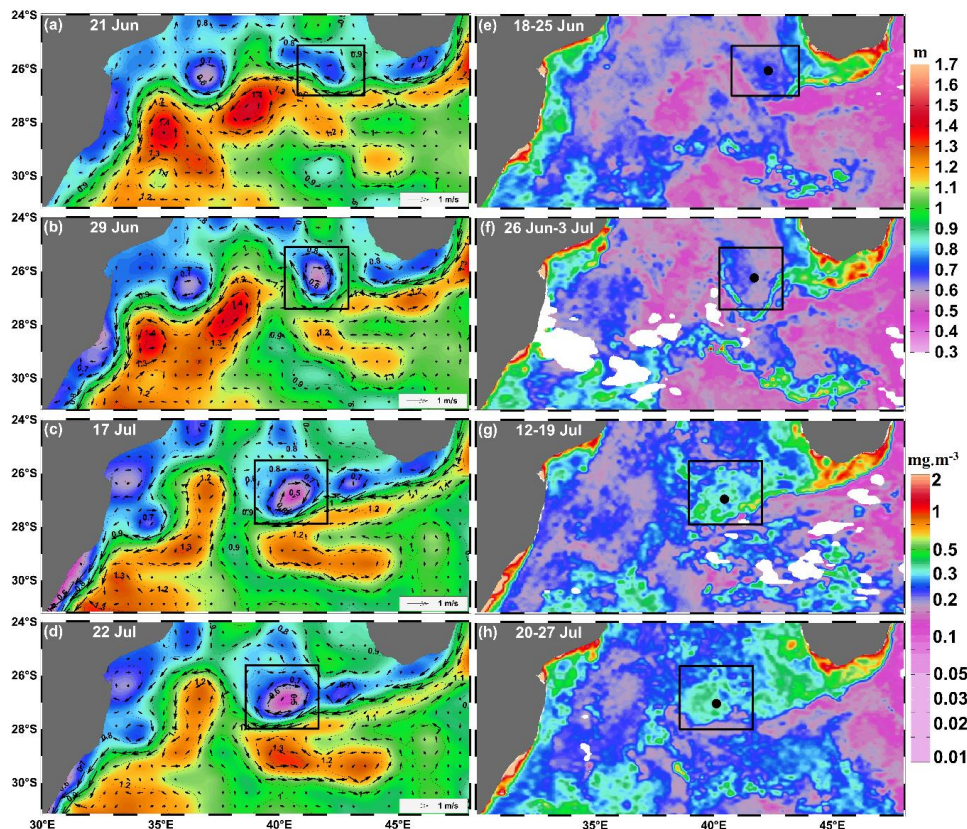
Figure 4. (**a–d**) Daily Sea Surface Height (colour contours) and geostrophic velocity (black arrows) on selected days for 21 June to 22 July 2013; and (**e–h**) 8-day MODIS Aqua chlorophyll *a* composites for 18 June to 27 July 2013, over the Mozambique Basin. Black boxes highlight the location of the cyclonic eddy and black dots indicate the centre of the eddy. White areas indicate missing data due to cloud cover.

Elevated chlorophyll *a* was observed across the southern shelf of Madagascar (26–26.5°S; 44–47°E; Figure 4e). Some of this elevated chlorophyll *a* appears to be advected from the shelf along the northern edge of the SEMC flow towards the eddy (Figure 4e,f,) and then entrained around the perimeter of the eddy by the cyclonic flow during 26 June to 3 July (Figure 4f). Chlorophyll *a* levels had increased to 0.4–0.6 mg·m^{-3} within the eddy by 12–19 July, with slightly higher values along the southern perimeter (Figure 4g). Elevated chlorophyll *a* levels within the eddy were maintained through 20–27 July (Figure 4h).

Total chlorophyll *a* on the southern shelf of Madagascar for the period 18 June to 27 July, while picophytoplankton contributed <20% (Figure 5). Similarly, nano- and picophytoplankton comprised the community within the cyclonic eddy over the period 18 June to 3 July but the micro- and nanophytoplankton proportions increased around the periphery of the eddy during 26 June to 3 July

(Figure 5b). Micro- and nanophytoplankton continued to increase within the eddy during 12–19 July and 20–27 July (Figure 5c,d), with the highest proportion being located around the southern sector over 12–19 July (Figure 5c). The fractional contribution of picophytoplankton declined over 12–19 July and 20–27 July (Figure 5k,l) as the micro- and nanophytoplankton proportions increased.

The fractional contribution indicated that nano- and microphytoplankton contributed most. The eddy continued to move further west during August 2013, growing in size as it matured and merged with other cyclonic features, to reach 27°S; 38°E by 24 August (Figure 6a–d). Geostrophic velocity was maintained at 0.5–1 m·s^{-1} and the SSH at the core declined to a minimum of 0.38 m, after smaller cyclonic eddies to the north and east merged with the eddy in question (Figure 6b,c). Patchy distribution of chlorophyll *a* within the eddy was observed over 28 July to 12 August and chlorophyll-rich water still seemed to be transported from the southern Madagascar shelf to the eddy (Figure 6e,f). By 13–28 August, chlorophyll *a* within the eddy had declined to 0.2–0.3 mg·m^{-3} (Figure 6g,h). Fractional analysis showed that there was still some microphytoplankton within the eddy during 28 July to 12 August, but this size fraction declined to less than 15% thereafter (Figure 7a–d). Nanophytoplankton was the dominant fraction in the eddy during August 2013 (Figure 7e–h), but the picophytoplankton contribution increased from ~35% in the first half of August to ~40% in the second half (Figure 7i–l).

Southwesterly propagation of the eddy continued through September to mid-October 2013, moving from 27°S; 37.2°E on 1 September to 28.3°S; 34.1°E by 11 October, close to the Agulhas Current system off the east coast of South Africa (Figure 8a–d). The eddy appeared to be in a declining phase over this period as it decreased in size during its movement towards southern Africa (Figure 8a–d). Chlorophyll *a* levels in the eddy decreased from ~0.25 mg·m^{-3} to 0.15 mg·m^{-3} over this period, being similar to the surrounding waters in the western sector of the MB (Figure 8e–h). The microphytoplankton fraction in the eddy was very low (Figure 9a–d), with nanophytoplankton declining (Figure 9e,f) and the picophytoplankton contribution increasing throughout September (Figure 9i,j). In October, the nanophytoplankton contribution declined further (Figure 9g,h) and picophytoplankton was then the dominant fraction within the eddy (Figure 9k,l).
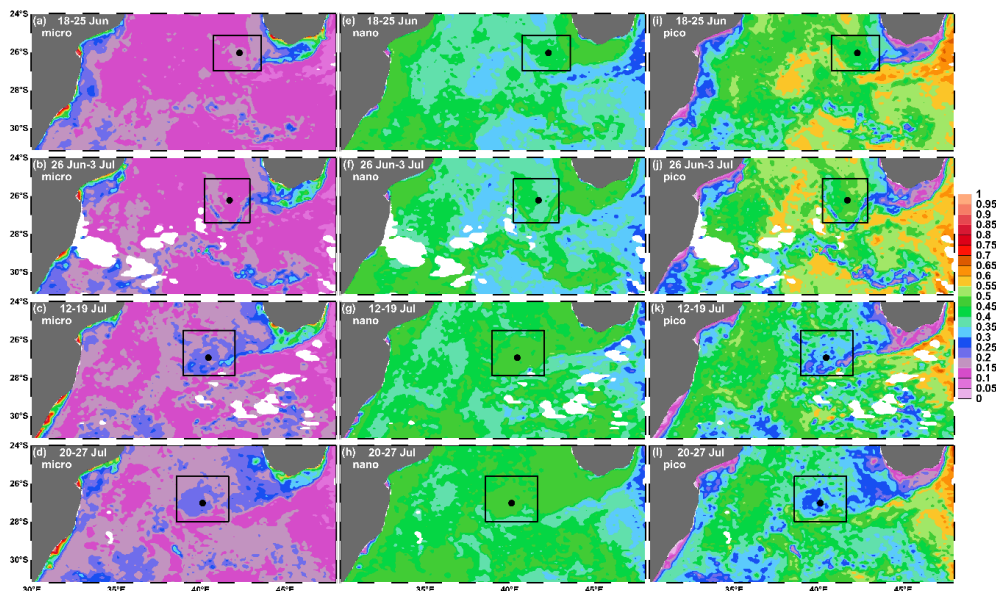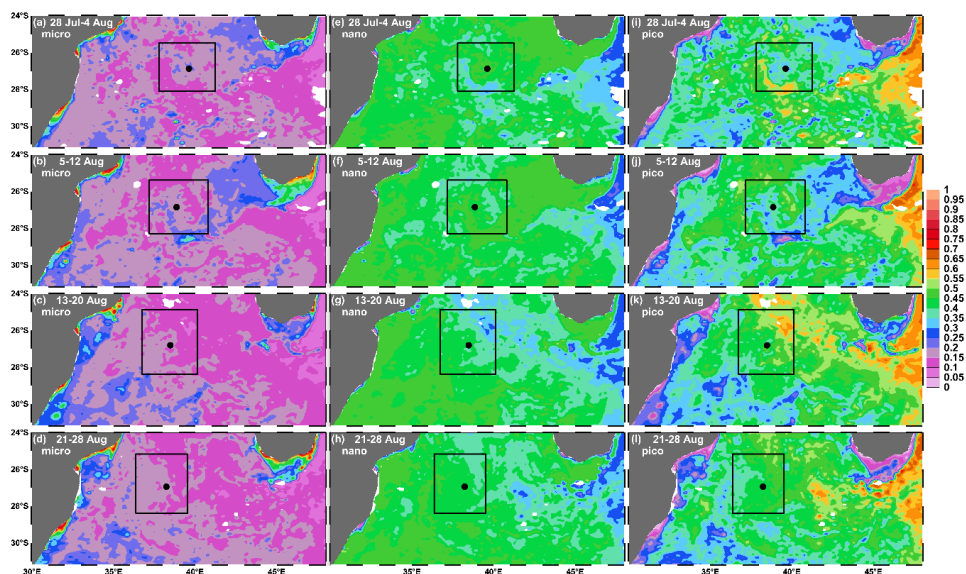

Figure 5. Fractional contribution of (**a**–**d**) micro-, (**e**–**h**) nano-, and (**i**–**l**) picophytoplankton to MODIS Aqua chlorophyll *a* for 18 June to 27 July 2013 over the Mozambique Basin. Black boxes highlight the location of the cyclonic eddy and black dots indicate the centre of the eddy. White areas indicate missing data due to cloud cover.
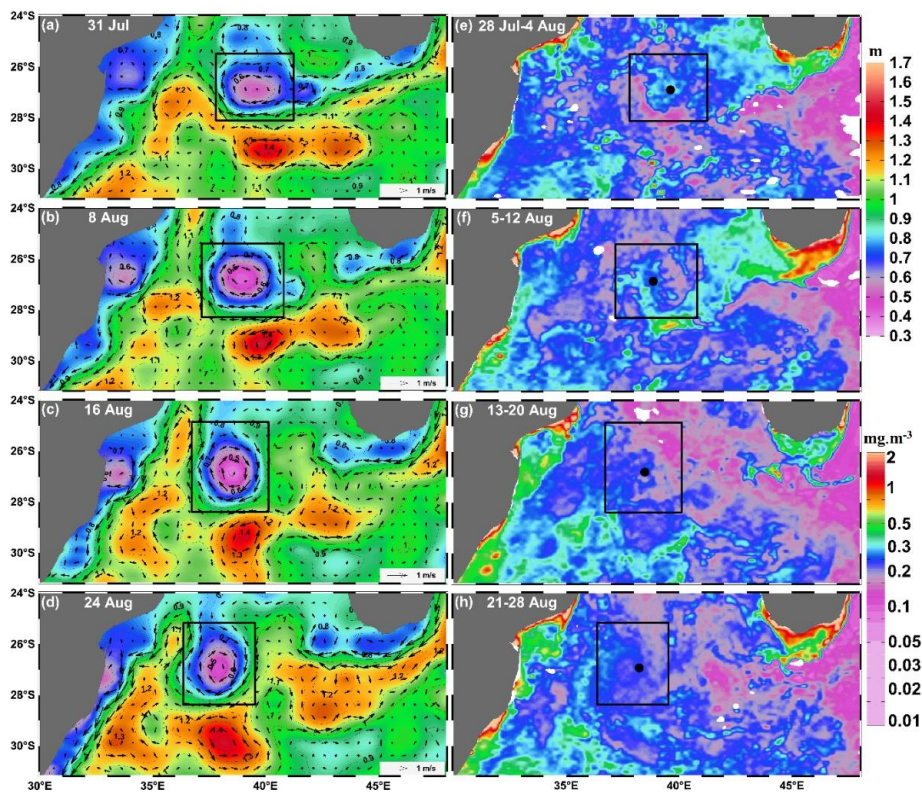
Figure 6. (**a**–**d**) Daily Sea Surface Height (colour contours) and geostrophic velocity (black arrows) on selected days for 31 July to 24 August 2013; and (**e**–**h**) 8-day MODIS Aqua chlorophyll *a* composites for 28 July to 28 August 2013, over the Mozambique Basin. Black boxes highlight the location of the cyclonic eddy and black dots indicate the centre of the eddy. White areas indicate missing data due to cloud cover.
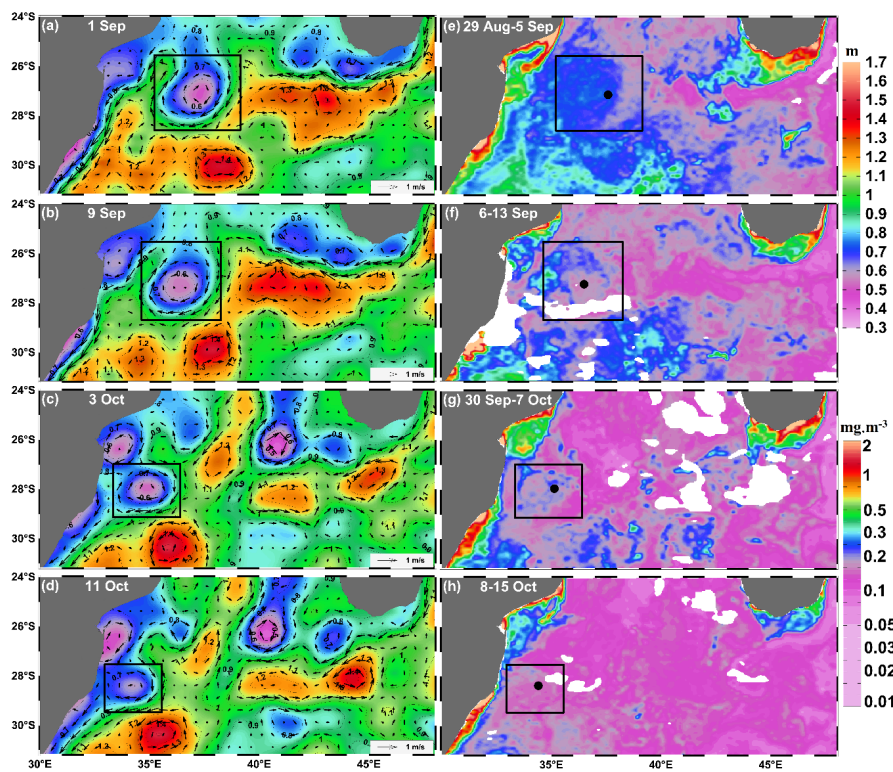

Figure 7. Fractional contribution of (**a**–**d**) micro-, (**e**–**h**) nano-, and (**i**–**l**) picophytoplankton to MODIS Aqua chlorophyll *a* for 28 July to 28 August 2013 over the Mozambique Basin. Black boxes highlight the location of the cyclonic eddy and black dots indicate the centre of the eddy. White areas indicate missing data due to cloud cover.

Figure 8. (**a**–**d**) Daily Sea Surface Height (colour contours) and geostrophic velocity (black arrows) on selected days for 1 September to 11 October 2013; and (**e**–**h**) 8-day MODIS Aqua chlorophyll *a* composites for 29 August to 15 October 2013, over the Mozambique Basin. Black boxes highlight the location of the cyclonic eddy and black dots indicate the centre of the eddy. White areas indicate missing data due to cloud cover.
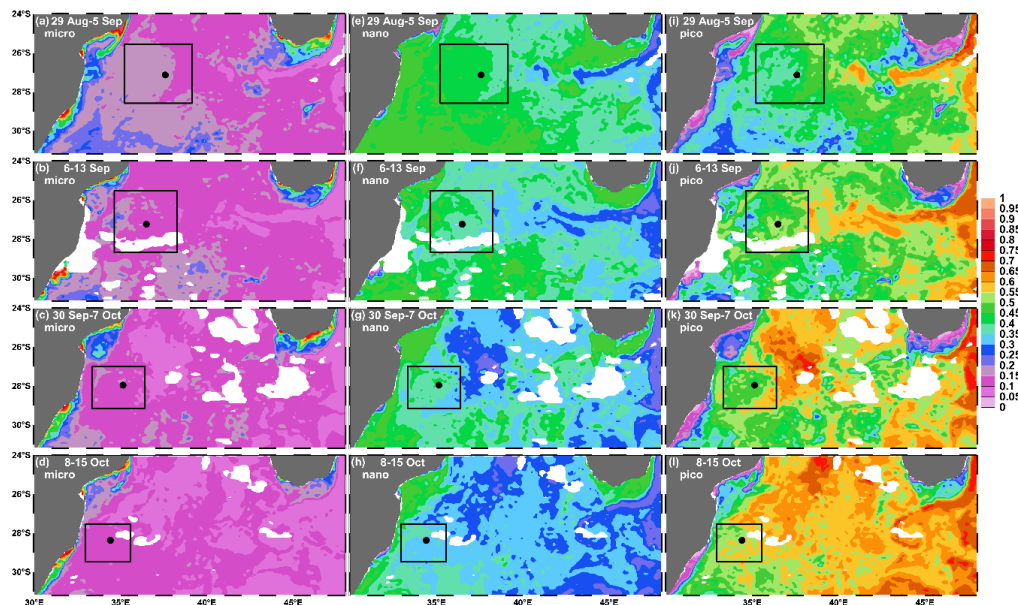
Figure 9. Fractional contribution of (**a**–**d**) micro-, (**e**–**h**) nano-, and (**i**–**l**) picophytoplankton to MODIS Aqua chlorophyll *a* for 29 August to 15 October 2013 over the Mozambique Basin. Black boxes highlight the location of the cyclonic eddy and black dots indicate the centre of the eddy. White areas indicate missing data due to cloud cover.

Figure 10 shows more detail of the temporal changes in the eddy as it propagated across the MB. The SSH was 0.76 m at the centre when the eddy was formed on 17 June 2013 and decreased steadily to 0.47 m by 22 July. Between 22 July and 5 August, a small increase to 0.53 m was observed (Figure 10a), after which SSH declined sharply to a minimum of 0.38 m on 15 August. This was followed by a steady increase to 0.55 m on 8–11 September. A further decrease in SSH to 0.46 m on 23–26 September occurred, and then SSH increased again to 0.6 m by 11 October and remained stable until the last day (18 October) the eddy was detected (Figure 10a). The mean 8-day chlorophyll *a* levels at the centre of the eddy were 0.21–0.22 mg·m^{-3} for 18–21 June and 26 June to 3 July, but increased to a maximum of 0.36 mg·m^{-3} by 20–27 July 2013 (Figure 10a). Chlorophyll *a* then decreased steadily to 0.24 mg·m^{-3} (21–28 August), followed by a slight increase to 0.26 mg·m^{-3} (29 August to 5 September), before it continued to decline, reaching 0.14 mg·m^{-3} by 8–15 October (Figure 10a). The size fractionation indicated that pico- and nanophytoplankton comprised most of the community in the centre of the eddy in June 2013, with the nano- fraction becoming dominant through July and August, and the picophytoplankton then dominating in September and October (Figure 10b). The microphytoplankton contribution was low overall and reached a maximum proportion of 23% over 20–27 July when the maximum chlorophyll *a* level was observed in the eddy (Figure 10b).
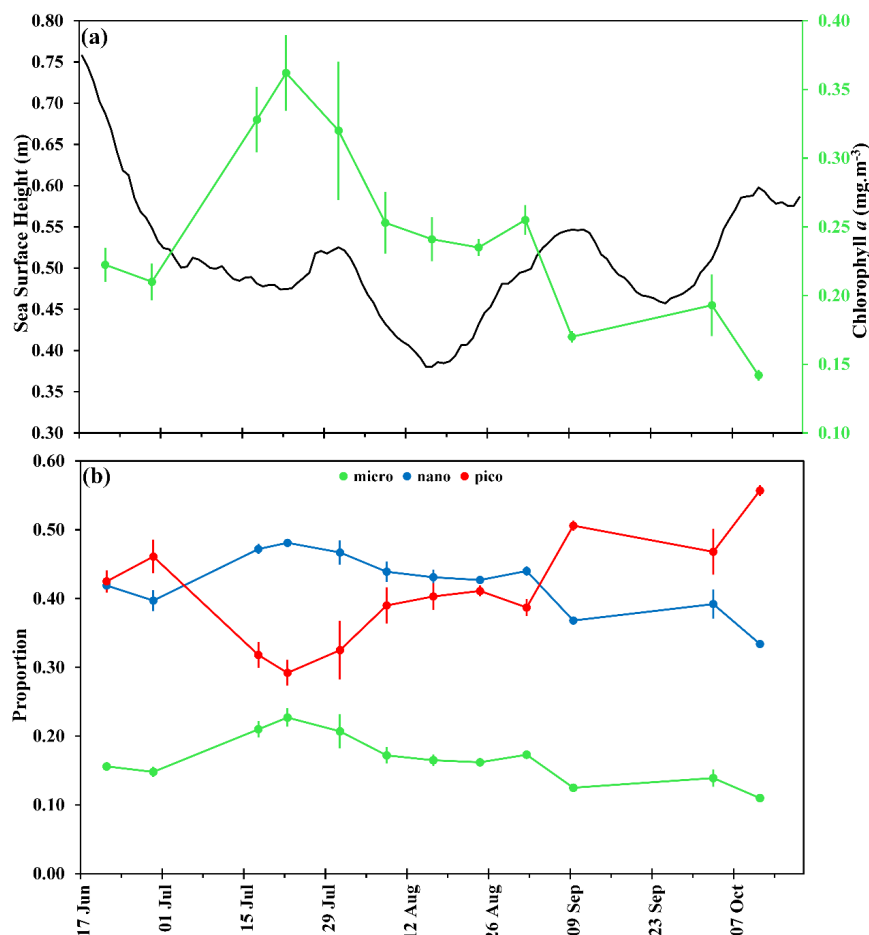
Figure 10. Temporal variation in (**a**) daily Sea Surface Height (SSH) (black line) and 8-day MODIS Aqua chlorophyll *a* (green line and dots), and (**b**) the fractional contribution of micro-, nano-, and picophytoplankton at the centre of the cyclonic eddy as it propagated across the Mozambique Basin. Vertical bars indicate the standard deviation of chlorophyll *a* and the fractional contributions of micro- (green dots and line), nano- (blue dots and line), and picophytoplankton (red dots and line) for the 3 × 3 pixel window at the centre of the eddy.

4. Discussion

Interest in the SEMC and eddies propagating across the Mozambique Basin (MB) stems from their role in transporting warm, salty Indian Ocean waters poleward into the Agulhas Current system, and their role in the shedding of rings into the Atlantic Ocean at the Agulhas Retroflection [3,32]. The formation, development and decline of the eddy over four months from mid-June until mid-October 2013 displayed interesting changes during its propagation across the MB. The SSH at the centre decreased steadily from its origin on 16 June until 21 July, after which it increased to 0.52 m on 31 July (Figure 10a). This increase was due to the influence of approaching smaller cyclonic eddies to the north and east of the MB eddy (Figures 4c,d and 6a) that eventually merged with the MB eddy (Figure 6b). The lowest SSH was observed on 15 and 16 August (Figure 10a) when the eddy reached its most intense state and had the largest diameter and surface area (Figure 6c). The increase in SSH thereafter (Figure 10a) indicated the decline of the eddy as its area decreased with the drift of the eddy further to the west (Figures 6d and 8a,b).

SSH reached another peak on 8–11 September (Figure 10a) and this was due to the influence of another small cyclonic eddy that drifted south from the Mozambique Channel (MC) to merge into the MB eddy (Figure 8a,b). The decrease in SSH during September reflected the intensification of the MB eddy after merging with the smaller cyclonic eddy from the Channel (Figure 8a,b), while the increase in SSH in October (Figure 10a), as well as the decrease in size (Figure 8c,d) indicated the dissipation of the MB eddy as it interacted with the Agulhas Current system along the east coast of South Africa (Figure 8d). These findings are in agreement with previous investigations which have shown that the characteristics of eddies within the region are well described by altimetry data [8,9,33], and the properties of the MB eddy, as well as the interactions with surrounding eddies, are similar to those defined in existing literature [3,6–11]. Our observations also agree with a more recent study that demonstrated the dissipation of eddies upon reaching the Agulhas Current due to eddy-current interactions [34].

The dynamics associated with mesoscale eddies have a significant influence on biological communities [12–14]. An in situ investigation of the MB eddy one month after its formation showed a uniform distribution of chlorophyll *a* in the upper 100 m [16], as a result of the well mixed nature of the water column under strong wind conditions [15,16]. CHEMTAX analysis of pigment data, which estimates the fractional contribution of phytoplankton functional groups to the total chlorophyll *a* according to an input matrix of pigment ratios, indicated a phytoplankton community comprising mainly haptophytes (nanophytoplankton) and diatoms (microphytoplankton), with diatoms being more prominent in the centre of the eddy, while greater proportions of prokaryotes (picophytoplankton) were found outside the eddy [16]. This was consistent with the application of the diagnostic pigment analysis for size structure [19,24] conducted here on the same samples (Figure 2). In contrast to the in situ data, the satellite data (Figure 2) coinciding with the research cruise indicated slightly lower contributions by microphytoplankton and slightly higher proportions of nanophytoplankton in the eddy (Figure 2f,g).

These discrepancies likely result from three reasons: (1) slight deviations from the Lamont et al. [19] parameterization in the relationships between micro- (higher) and nanophytoplankton (lower) size fractions for a given chlorophyll *a* concentration (Figure 2a,b); (2) slightly lower satellite chlorophyll *a* concentrations used as input to the three-component model than in situ data in the eddy (Figure 2d–g); (3) differences in sampling resolution (both spatial and temporal) between the in situ data and the satellite data, with the in situ data capturing much higher frequency variations, while the coarser satellite data likely smooths much of these fluctuations. Nevertheless, the overall good correspondence between the in situ and the satellite observations of size classes in the MB eddy, and the fact that the majority of the samples from the in situ study lie within the uncertainty of the satellite model estimates (Figure 2), suggests that remote sensing of phytoplankton size classes is not only useful for investigations over larger spatial and temporal scales [18,19,22–24], but can also be effectively applied to studies of phytoplankton community structure in smaller ocean

features such as eddies. A similar study of phytoplankton size classes in an eddy in the South China Sea by Lin et al. [25] also demonstrated the utility of satellite-derived phytoplankton size structure in furthering the understanding of the biological impacts of mesoscale eddies.

In the MC to the north, in situ investigations revealed that cyclonic eddies had distinct subsurface chlorophyll maxima (SCMs) associated with shallow upper mixed layers and nitracline depths and deep euphotic zones during austral spring and summer [15], where prokaryotes (picophytoplankton) generally dominated at the surface and flagellates (nanophytoplankton) at the SCM [13,14]. The MB eddy was different in that it was sampled during austral winter, had a shallower euphotic zone, a deeper upper mixed layer and a uniform chlorophyll distribution throughout the euphotic zone [15,16]. Nano- and picophytoplankton comprised the community at the surface in the MB eddy during its early development during austral winter in June 2013 (Figures 5 and 10). As the eddy became more intense during July 2013, there was an increase in the microphytoplankton and a corresponding decline in the picophytoplankton proportion (Figures 5 and 10). It is not unusual for microphytoplankton in the form of diatoms to be prominent in deep sea eddies, as Brown et al. [35] and Rii et al. [36] have also observed diatom prominence in the centre of a Hawaiian cyclonic eddy. Similar to the MB eddy (Figures 5 and 10), which was approximately one month old at the time of sampling [15,16], the Hawaiian eddy was also ~one month old, and in a mature phase of its life cycle [35–37]. In contrast to the MB eddy (Figures 5 and 10), where phytoplankton was uniformly distributed throughout a deep upper mixed layer [15,16], the Hawaiian eddy had upper mixed layer populations dominated by picophytoplankton and a distinct SCM primarily comprised of large chain-forming diatoms [35,36]. Nencioli et al. [37] postulated that nutrient input into the eddy continued during its mature phase as a result of significant subsurface horizontal exchange of waters, thus promoting and sustaining diatom growth in the lower euphotic zone [35,36].

Conventional upwelling of nutrients into the euphotic zone did not appear to operate in the MB eddy, as the central doming did not penetrate into the upper 100 m and the upper mixed layer and nitracline depths were much deeper than the euphotic zone, suggesting limited vertical nutrient supply into the euphotic zone from below [15,16]. The microphytoplankton population in the eddy did not appear to be seeded and stimulated by internal upwelling processes. Instead, this population originated on the southern Madagascar shelf and was transported along the northern boundary of the enhanced westerly to southwesterly flow (Figure 5a,b) resulting from the eddy interactions to the southwest of Madagascar (Figures 3 and 4a–d). Interactions between the cyclonic eddy and the southwesterly flow resulted in the microphytoplankton being entrained into the outer boundary of the eddy (Figures 4a,b,e,f, and 5a,b) and then distributed throughout the upper water column within the eddy, probably due to a combination of eddy dynamics and strong wind-induced vertical mixing [15,16]. Due to its formation and development near the southern Madagascar shelf, the MB eddy was uniquely located to be seeded with microphytoplankton communities from the shelf by horizontal advection and subsequent vertical mixing, as opposed to the stimulation of the phytoplankton community by vertical upwelling fluxes.

This is in agreement with previous observations in this region which have demonstrated the advection of high chlorophyll waters from the shelf and subsequent entrainment into cyclonic eddies [38]. Similarly, remote sensing of phytoplankton has been used in the eastern Gulf of Alaska near northern Canada to illustrate highly productive coastal waters being advected offshore into the peripheries of anticyclonic eddies that form close to the Queen Charlotte Islands in boreal winter [39,40]. The seaward transport of phytoplankton can be swift and drifter measurements have revealed speeds of 0.25 m·s^{-1} along the outer portions of these eddies [41]. At such speeds, entrained coastal waters can be carried 100 km offshore in six days, which is within a few lifetimes of phytoplankton such as diatoms [39]. In the MC and MB, similar rapid drifter translation speeds have been observed in the frontal regions between mesoscale features, with highly variable transit durations from 15 to 113 days between Madagascar and Mozambique, off the southern African east coast [42]. The geostrophic velocity of the southwesterly flow between southern Madagascar and the

cyclonic eddy was 0.5–1 m·s^{-1} (Figures 3 and 4b,c), and it is estimated that phytoplankton from the southern Madagascar shelf could be transported between 300 km and 700 km within 7–8 days. It is likely that these velocities are underestimated since the altimetry data is gridded resulting in some features not being fully resolved, and ground tracks are not always perpendicular to the flow [43] and it has been shown that altimeter-derived geostrophic velocities were 30% weaker than in situ current measurements in the MC [44]. Nevertheless, such translation speeds mean that the micro- and nanophytoplankton advected from the Madagascar shelf would still be viable when entrained into the cyclonic eddy (Figure 4e,f), and could be sustained (Figure 4g,h) by a combination of access to nutrients through strong vertical mixing within the eddy [15,16], and by persistent advection from the shelf and entrainment into the eddy, as suggested by Figures 4g,h and 5c,d.

Chlorophyll *a* levels reached a peak during 20–27 July when the proportions of micro- and nanophytoplankton were maximum and picophytoplankton was at a minimum (Figures 4h and 10). Phytoplankton biomass then declined as indicated by the steady decrease in chlorophyll *a* (Figures 6e–h, 8e–h and 10a), while the community structure changed, with declining proportions of micro- and nanophytoplankton and an increasing contribution of picophytoplankton (Figures 7, 9, and 10b). There was a slight increase in chlorophyll *a*, micro- and nanophytoplankton during 29 August to 5 September (Figures 9a,e, and 10), and this may have been due to a contribution of biomass by the cyclonic eddy that drifted south from the MC to merge with the MB eddy (Figure 8a), as discussed above. In September and October, there was a substantial decrease in phytoplankton biomass (Figure 10) as the eddy drifted further to the southwest (Figure 8). A marked shift in community structure occurred during this time, where picophytoplankton became dominant as the contributions of micro- and nanophytoplankton decreased. In contrast to the current study, Lin et al. [25] observed that picophytoplankton was dominant throughout the life cycle of a cyclonic eddy in the South China Sea, where micro- and nanophytoplankton only reached maximum proportions of 24% and 30%, respectively. It must be noted that the Lin et al. study makes no mention of the translation of the eddy over large distances [25], as was observed in the current study (Figures 4–9). Their study [25] also does not note any interactions between the eddy and other surrounding mesoscale features, or shelf regions, as demonstrated above (Figures 4–9).

The focus of this investigation has been on the temporal changes in the MB eddy as it propagated southwestwards, but the phytoplankton community needs to be viewed in the overall context of the MB. Apart from the inclusion of microphytoplankton from the Madagascar shelf during July 2013 (Figures 4 and 5), the population within the eddy was largely similar to the surrounding waters (Figures 6, 7, and 9). Nanophytoplankton was mostly dominant both within the eddy (Figure 10) and across the MB during July and August, apart from some patchy zones where the pico-fraction was prominent (Figures 5 and 7). These are winter months in the southern Hemisphere, and Lamont et al. [19] has previously demonstrated that the nano- fraction usually dominates in the southern MC and throughout the MB during this season. The population began to change in September during early spring as picophytoplankton became more prominent in the eastern sector of the MB, and by October, the pico- fraction was more dominant across the MB (Figure 9). Similarly, it has previously been shown that picophytoplankton are dominant during summer months in this region, while mixed communities of pico- and nanophytoplankton prevail during autumn and spring [19].

Thus, besides the input of microphytoplankton from the Madagascar shelf in July 2013 (Figures 4 and 5), and the small short-term increase in the micro- and nanophytoplankton proportions after merging with another eddy at the end of August (Figures 8a and 10), temporal changes in community structure observed during the eddy's ~four-month lifetime resembled previously described seasonal variations in size structure in the region [19]. Previous investigations in the open ocean of the Pacific and Atlantic have indicated that cyclonic eddies can increase their phytoplankton biomass and photosynthetic activity early in their development but upwelling at the centre usually results in an increase in biomass and a change in photophysiology at the SCM, but not in the water column above the SCM [45]. Consequently, such biological responses at depth cannot be accurately determined by

remote sensing, but only by in situ measurements. However, as demonstrated in the current study, among others [18–20,22–25], ocean colour measurements are still useful for investigating variations in surface phytoplankton populations over a range of spatial and temporal scales. Although it was clearly demonstrated that phytoplankton biomass was uniformly distributed throughout the upper mixed layer of the eddy in July 2013 [15,16] and that satellite observations during this time (Figures 4 and 5) were in good agreement with in situ measurements [15,16] (also see Figure 2), it is possible that the vertical distribution of phytoplankton changed such that SCMs developed during the translation of the cyclonic eddy across the MB. Such a change would signify a seasonal transition from well mixed upper layers in winter to more stratified conditions in summer and would be in accordance with the findings of Lamont et al. [15], who demonstrated that cyclonic eddies sampled during spring and summer had distinct SCMs while the opposite was true for those sampled in winter.

5. Conclusions

The application of the three-component model of Brewin et al. [18] to satellite ocean colour data has proven to be useful for tracking the surface phytoplankton community within a cyclonic eddy as it propagated across the MB over a four-month period from mid-June to mid-October 2013. This is the first study to investigate the temporal changes in community structure within an eddy that moves across an ocean basin in the southwest Indian Ocean, and useful quantitative information was obtained on the variability of chlorophyll *a* levels and the proportions of micro-, nano-, and picophytoplankton. Although the community within the eddy was generally similar to the population in the surrounding waters of the MB, in the early stage of development, the eddy was seeded with microphytoplankton from the southern Madagascar shelf by horizontal advection and subsequent entrainment, rather than by vertical uplift of nutrient-rich waters into the euphotic zone as is common in cyclonic eddies. This was due to the particular location of the eddy close to the Madagascar shelf, as well as the spatial structuring of surrounding mesoscale features which served to enhance southwestward flow around the southern tip of Madagascar and export of waters from the shelf.

Overall, the community within the propagating eddy and across the MB was dominated by nanophytoplankton during the austral winter months of July and August, but this changed to picophytoplankton dominance in austral spring during September and October. This suggested that, besides the injection of shelf waters and phytoplankton communities during the interaction of the eddy with the southern Madagascar shelf in July 2013, the most prominent changes in surface phytoplankton communities over the four-month lifetime of the eddy were associated with the seasonal variations from winter to spring and summer. Apart from the satellite observations, there are no phytoplankton measurements within the eddy subsequent to the research cruise in July 2013 [15,16] and thus it is not possible to verify using in situ data if such changes indeed took place. Furthermore, additional research in the form of more well-designed in situ studies, together with more detailed and directed analysis of satellite observations and model output, are required to determine if the pattern of variability described in the current study was unique to the MB eddy, or whether it is typical of all long-lived cyclonic eddies within the region.

Author Contributions: T.L. designed the project, conceived and performed the data analysis, and prepared the figures. R.J.W.B. contributed to the data analysis and preparation of figures. T.L., R.G.B. and R.J.W.B. shared the interpretation of the data and the writing of the article.

References

1. Swallow, J.; Fieux, M.; Schott, F. The boundary currents east and north of Madagascar: 1. Geostrophic currents and transports. *J. Geophys. Res.* **1988**, *93*, 4951–4962. [CrossRef]
2. Nauw, J.J.; van Aken, H.M.; Webb, A.; Lutjeharms, J.R.E.; de Ruijter, W.P.M. Observations of the southern east Madagascar current and undercurrent and countercurrent system. *J. Geophys. Res.* **2008**, *113*. [CrossRef]
3. Ridderinkhof, W.; Le Bars, D.; von der Heydt, A.S.; de Ruijter, W.P.M. Dipoles of the South-East Madagascar Current. *Geophys. Res. Lett.* **2013**, *40*, 558–562. [CrossRef]
4. Siedler, G.; Rouault, M.; Lutjeharms, J.R.E. Structure and origin of the subtropical South Indian Ocean Countercurrent. *Geophys. Res. Lett.* **2006**, *33*. [CrossRef]
5. Siedler, G.; Rouault, M.; Biastoch, A.; Backeberg, B.; Reason, C.J.C.; Lutjeharms, J.R.E. Modes of the southern extension of the East Madagascar Current. *J. Geophys. Res.* **2009**, *114*. [CrossRef]
6. De Ruijter, W.P.M.; van Aken, H.M.; Beier, E.J.; Lutjeharms, J.R.E.; Matano, R.P.; Schouten, M.W. Eddies and dipoles around South Madagascar: Formation, pathways and large-scale impact. *Deep Sea Res. Part I* **2004**, *51*, 383–400. [CrossRef]
7. Chapman, P.; Di Marco, S.F.; Davis, R.E.; Coward, A.C. Flow at intermediate depths around Madagascar based on ALACE float trajectories. *Deep Sea Res. Part II* **2003**, *50*, 1957–1986. [CrossRef]
8. Halo, I.; Backeberg, B.; Penven, P.; Ansorge, I.; Reason, C.; Ullgren, J.E. Eddy properties in the Mozambique Channel: A comparison between observations and two numerical ocean circulation models. *Deep Sea Res. Part II* **2014**, *100*, 38–53. [CrossRef]
9. Halo, I.; Penven, P.; Backeberg, B.; Ansorge, I.; Shillington, F.; Roman, R. Mesoscale eddy variability in the southern extension of the East Madagascar Current: Seasonal cycle, energy conversion terms, and eddy mean properties. *J. Geophys. Res. Oceans* **2014**, *119*, 7324–7356. [CrossRef]
10. Quartly, G.D.; Buck, J.J.H.; Srokosz, M.A.; Coward, A.C. Eddies around Madagascar—The retroflection re-considered. *J. Mar. Syst.* **2006**, *63*, 115–129. [CrossRef]
11. De Ruijter, W.P.; Ridderinkhof, H.; Schouten, M.W. Variability of the southwest Indian Ocean. *Philos. Trans. R. Soc.* **2005**, *363*, 63–76. [CrossRef] [PubMed]
12. Tew-Kai, E.; Marsac, F. Patterns of variability of sea surface chlorophyll in the Mozambique Channel: A quantitative approach. *J. Mar. Syst.* **2009**, *77*, 77–88. [CrossRef]
13. Barlow, R.; Lamont, T.; Morris, T.; Sessions, H.; van den Berg, M. Adaptation of phytoplankton communities to mesoscale eddies in the Mozambique Channel. *Deep Sea Res. Part II* **2014**, *100*, 106–114. [CrossRef]
14. Lamont, T.; Barlow, R.G.; Morris, T.; van den Berg, M.A. Characterisation of mesoscale features and phytoplankton variability in the Mozambique Channel. *Deep Sea Res. Part II* **2014**, *100*, 94–105. [CrossRef]
15. Lamont, T.; Barlow, R.G. Contrasting hydrography and phytoplankton distribution in the upper layers of cyclonic eddies in the Mozambique Basin and Mozambique Channel. *Afr. J. Mar. Sci.* **2017**, *39*, 239–306. [CrossRef]
16. Barlow, R.; Lamont, T.; Gibberd, M.-J.; Airs, R.; Jacobs, L.; Britz, K. Phytoplankton communities and acclimation in a cyclonic eddy in the southwest Indian Ocean. *Deep Sea Res. Part I* **2017**, *124*, 18–30. [CrossRef]
17. IOCCG. *Phytoplankton Functional Types from Space*; Sathyendranath, S., Ed.; Reports of the International Ocean-Colour Coordinating Group, No. 15, IOCCG; IOCCG: Dartmouth, NS, Canada, 2014.
18. Brewin, R.J.W.; Sathyendranath, S.; Hirata, T.; Lavender, S.J.; Barciela, R.M.; Hardman-Mountford, N.J. A three-component model of phytoplankton size class for the Atlantic Ocean. *Ecol. Model.* **2010**, *221*, 1472–1483. [CrossRef]
19. Lamont, T.; Brewin, R.J.W.; Barlow, R.G. Seasonal variation in remotely-sensed phytoplankton size structure around southern Africa. *Remote Sens. Environ.* **2018**, *204*, 617–631. [CrossRef]
20. Sathyendranath, S.; Cota, G.; Stuart, V.; Maass, H.; Platt, T. Remote sensing of phytoplankton pigments: A comparison of empirical and theoretical approaches. *Int. J. Remote Sens.* **2001**, *22*, 249–273. [CrossRef]
21. Uitz, J.; Claustre, H.; Morel, A.; Hooker, S.B. Vertical distribution of phytoplankton communities in the open ocean: An assessment based on surface chlorophyll. *J. Geophys. Res.* **2006**, *111*. [CrossRef]
22. Devred, E.; Sathyendranath, S.; Stuart, V.; Platt, T. A three component classification of phytoplankton absorption spectra: Application to ocean-colour data. *Remote Sens. Environ.* **2011**, *115*, 2255–2266. [CrossRef]

23. Brewin, R.J.W.; Hirata, T.; Hardman-Mountford, N.J.; Lavender, S.J.; Sathyendranath, S.; Barlow, R. The influence of the Indian Ocean Dipole on interannual variations in phytoplankton size structure as revealed by Earth Observation. *Deep Sea Res. Part II* **2012**, *77–80*, 117–127. [CrossRef]

24. Brewin, R.J.W.; Sathyendranath, S.; Jackson, T.; Barlow, R.; Brotas, V.; Airs, R.; Lamont, T. Influence of light in the mixed-layer on the parameters of a three-component model of phytoplankton size class. *Remote Sens. Environ.* **2015**, *168*, 437–450. [CrossRef]

25. Lin, J.; Cao, W.; Wang, G.; Hu, S. Satellite-observed variability of phytoplankton size classes associated with a cold eddy in the South China Sea. *Mar. Pollut. Bull.* **2014**, *83*, 190–197. [CrossRef] [PubMed]

26. Bailey, S.W.; Werdell, P.J. A multi-sensor approach for the on-orbit validation of ocean color satellite data products. *Remote Sens. Environ.* **2006**, *102*, 12–23. [CrossRef]

27. Brewin, R.J.W.; Dall'Olmo, G.; Pardo, S.; van Dongen-Vogels, V.; Boss, E.S. Underway spectrophotometry along the Atlantic Meridional Transect reveals high performance in satellite chlorophyll retrievals. *Remote Sens. Environ.* **2016**, *183*, 82–97. [CrossRef]

28. DUACS/AVISO Team. A New Version of SSALTO/Duacs Products Available in April 2014. Version 1.1, Centre National d'Etudes Spatiales. Available online: https://www.aviso.altimetry.fr/fileadmin/documents/data/duacs/Duacs2014.pdf (accessed on 7 March 2018).

29. Nasa Goddard Space Flight Center; Ocean Ecology Laboratory; Ocean Biology Processing Group. *Moderate-Resolution Imaging Spectroradiometer (MODIS) Aqua Chlorophyll Data*; 2018 Reprocessing; NASA OB.DAAC: Greenbelt, MD, USA, 2018. [CrossRef]

30. Aiken, J.; Fishwick, J.R.; Lavender, S.; Barlow, R.; Moore, G.F.; Sessions, H.; Bernard, S.; Ras, J.; Hardman-Mountford, N.J. Validation of MERIS reflectance and chlorophyll during the BENCAL cruise October 2002: Preliminary validation of new demonstration products for phytoplankton functional types and photosynthetic parameters. *Int. J. Remote Sens.* **2007**, *28*, 497–516. [CrossRef]

31. Barlow, R.; Stuart, V.; Lutz, V.; Sessions, H.; Sathyendranath, S.; Platt, T.; Kyewalyanga, M.; Clementson, L.; Fukasawa, M.; Watanabe, S.; et al. Seasonal pigment patterns of surface phytoplankton in the subtropical southern hemisphere. *Deep Sea Res. Part I* **2007**, *54*, 1687–1703. [CrossRef]

32. Beal, L.M.; de Ruijter, W.P.M.; Biastoch, A.; Zahn, R. SCOR/WCRP/IAPSO Working Group 136. On the role of the Agulhas system in ocean circulation and climate. *Nature* **2011**, *472*, 429–436. [CrossRef] [PubMed]

33. Chelton, D.B.; Schlax, M.G.; Samelson, R.M. Global observations of nonlinear mesoscale eddies. *Prog. Oceanogr.* **2011**, *91*, 167–216. [CrossRef]

34. Braby, L.; Backeberg, B.C.; Ansorge, I.; Roberts, M.J.; Krug, M.; Reason, C.J.C. Observed eddy dissipation in the Agulhas Current. *Geophys. Res. Lett.* **2016**, *43*, 8143–8150. [CrossRef]

35. Brown, S.L.; Landry, M.R.; Selph, K.E.; Yang, E.J.; Rii, Y.M.; Bidigare, R.R. Diatoms in the desert: Plankton community response to a mesoscale eddy in the subtropical North Pacific. *Deep Sea Res. Part II* **2008**, *55*, 1321–1333. [CrossRef]

36. Rii, Y.M.; Brown, S.L.; Nencioli, F.; Kuwahara, V.; Dickey, T.; Karl, D.M.; Bidigare, R.R. The transient oasis: Nutrient-phytoplankton dynamics and particle export in Hawaiian lee cyclones. *Deep Sea Res. Part II* **2008**, *55*, 1275–1290. [CrossRef]

37. Nencioli, F.; Kuwahara, V.S.; Dickey, T.D.; Rii, Y.M.; Bidigare, R.R. Physical dynamics and biological implications of a mesoscale eddy in the lee of Hawaii: Cyclone Opal observations during E-Flux III. *Deep Sea Res. Part II* **2008**, *55*, 1252–1274. [CrossRef]

38. Quartly, G.D.; Srokosz, M.A. Eddies in the southern Mozambique Channel. *Deep Sea Res. Part II* **2004**, *51*, 69–83. [CrossRef]

39. Crawford, W.R.; Brickley, P.J.; Peterson, T.D.; Thomas, A.C. Impact of Haida eddies on chlorophyll distribution in the Eastern Gulf of Alaska. *Deep Sea Res. Part II* **2005**, *52*, 975–989. [CrossRef]

40. Batten, S.D.; Crawford, W.R. The influence of coastal origin eddies on oceanic plankton distributions in the eastern Gulf of Alaska. *Deep Sea Res. Part II* **2005**, *52*, 991–1009. [CrossRef]

41. Yelland, D.; Crawford, W.R. Currents in Haida Eddies. *Deep Sea Res. Part II* **2005**, *52*, 875–892. [CrossRef]

42. Marsac, F.; Barlow, R.; Ternon, J.F.; Ménard, F.; Roberts, R. Ecosystem functioning in the Mozambique Channel: Synthesis and future research. *Deep Sea Res. Part II* **2014**, *100*, 212–220. [CrossRef]

43. Backeberg, B.C.; Johannessen, J.A.; Bertino, L.; Reason, C.J.C. The greater Agulhas Current system: An integrated study of its mesoscale variability. *J. Oper. Oceanogr.* **2008**, *1*, 29–44. [CrossRef]

44. Ternon, J.F.; Roberts, M.J.; Morris, T.; Hanke, L.; Backeberg, B. In situ measured current structures of the eddy field in the Mozambique Channel. *Deep Sea Res. Part II* **2014**, *100*, 10–26. [CrossRef]

45. Bibby, T.S.; Gorbunov, M.Y.; Wyman, K.W.; Falkowski, P.G. Photosynthetic community responses to upwelling in mesoscale eddies in the subtropical North Atlantic and Pacific Oceans. *Deep Sea Res. Part II* **2008**, *55*, 1310–1320. [CrossRef]